**Atmospheric
Measurement
Techniques
Discussions**

MODIS 3 km aerosol product: algorithm and global perspective

L. A. Remer[1], S. Mattoo[2,3], R. C. Levy[2,3], and L. Munchak[2,3]

[1]Joint Center for Earth Systems Technology (JCET), University of Maryland
Baltimore County (UMBC), Baltimore MD 21228, USA
[2]Climate and Radiation Laboratory, NASA Goddard Space Flight Center,
Greenbelt MD 20771, USA
[3]Science Systems and Applications, Inc., Lanham MD 20709, USA

Correspondence to: L. A. Remer (laremer@hotmail.com)

Discussion Paper | Discussion Paper | Discussion Paper | Discussion Paper |

AMTD

6, 69–112, 2013

MODIS 3 km aerosol product: algorithm and global perspective

L. A. Remer et al.

Title Page

Abstract	Introduction
Conclusions	References
Tables	Figures

|◄ | ►|
◄ | ►

Back | Close

Full Screen / Esc

Printer-friendly Version

Interactive Discussion

Abstract

After more than a decade of producing a nominal 10 km aerosol product based on the dark target method, the MODIS aerosol team will be releasing a nominal 3 km product as part of their Collection 6 release. The new product differs from the original 10 km product only in the manner in which reflectance pixels are ingested, organized and selected by the aerosol algorithm. Overall, the 3 km product closely mirrors the 10 km product. However, the finer resolution product is able to retrieve over ocean closer to islands and coastlines, and is better able to resolve fine aerosol features such as smoke plumes over both ocean and land. In some situations, it provides retrievals over entire regions that the 10 km product barely samples. In situations traditionally difficult for the dark target algorithm, such as over bright or urban surfaces the 3 km product introduces isolated spikes of artificially high aerosol optical depth (AOD) that the 10 km algorithm avoids. Over land, globally, the 3 km product appears to be 0.01 to 0.02 higher than the 10 km product, while over ocean, the 3 km algorithm is retrieving a proportionally greater number of very low aerosol loading situations. Based on collocations with ground-based observations for only six months, expected errors associated with the 3 km land product are determined to be greater than for the 10 km product: $\pm 0.05 \pm 0.25$ AOD. Over ocean, the suggestion is for expected errors to be the same as the 10 km product: $\pm 0.03 \pm 0.05$ AOD. The advantage of the product is on the local scale, which will require continued evaluation not addressed here. Nevertheless, the new 3 km product is expected to provide important information complementary to existing satellite-derived products and become an important tool for the aerosol community.

1 Introduction

The MODerate resolution Imaging Spectroradiometer (MODIS) has been observing the Earth from the Terra satellite since 2000 and from the Aqua satellite since 2002.

Among the many physical parameters derived from MODIS spectral radiances are a suite of products characterizing aerosol particles. There are several algorithms producing aerosol products from MODIS. In this paper we address the pair of algorithms referred to as the Dark Target algorithms, over land and ocean (Remer et al., 2005; Levy et al., 2007a, b, 2010). The original motivation behind the development of the Dark Target algorithms was to provide the necessary information to quantify aerosol effect on climate and climate processes, and thereby narrow uncertainties in estimating climate change (Kaufman et al., 1997, 2002; Tanré et al., 1997). Indeed in the subsequent dozen years since Terra launch, the scientific literature abounds in references to MODIS aerosol products to estimate direct aerosol effects (Remer et al., 2006; Yu et al., 2006) including the anthropogenic portion (Kaufman et al., 2005a; Christopher et al., 2006), to constrain climate models in their efforts to simulate climate processes (Stier et al., 2005; Kinne et al., 2006), to estimate intercontinental transport of aerosol (Kaufman et al., 2005b; Yu et al., 2012) and to further our understanding of aerosol-cloud-precipitation processes (Kaufman et al., 2005c; Koren et al., 2005; Koren and Wang, 2008; Loeb and Schuster, 2008).

The fundamental scale of the MODIS Dark Target aerosol product is 10 km at nadir that expands roughly four-fold towards the edges of the swath. This aerosol product is labeled Level 2. The Level 2 data follow the orbital path of the sensor and are not gridded. Instead each retrieval is labeled by the latitude-longitude of its center.

The Level 2 product is widely used to characterize local events, collocate with correlative data on a local level (Redemann et al., 2009; Russell et al., 2007), and to exert control on how the data are aggregated up to a coarser grid (Zhang et al., 2008.) Level 2 data are automatically aggregated to a $1° × 1°$ global grid, labeled Level 3 and made available to the community for global-scale applications.

One unexpected application of the MODIS Dark Target aerosol product is its use as a proxy for particulate pollution by the air quality community (Chu et al., 2003; Wang and Christopher 2003; Engel-Cox et al., 2004). The interest in using MODIS aerosol products to characterize air pollution has progressed both in the research arena (van

Donkelaar et al., 2006, 2010), and on the operational side (Al Saadi et al., 2005). The air quality community, except those interested in long-range and intercontinental transport of pollution (Yu et al., 2008), almost exclusively uses the Level 2 data product. Their interest requires identifying local areas of exposure and resolving gradients across an urban landscape. The 1-degree global grid is insufficient. Even though the air quality community uses the 10 km Level 2 product, there has been strong advocacy from that community and from others for a finer resolution product. Studies and applications besides air quality that would benefit from a finer resolution product include those characterizing smoke plumes from fires, those resolving aerosol loading in complex terrain and those interested in aerosol-cloud processes.

Alternative aerosol retrieval algorithms have been applied to MODIS data that produce a finer resolution product. Most of these have been local in scope, specifically tuned for the local area of interest (Li, C-C. et al., 2005; Castanho et al., 2008). A few have been applied to a more general global retrieval over land (Hsu et al., 2004; Lyapustin et al., 2011). These finer resolution retrievals, mostly at 1 km, show much promise in resolving individual smoke and pollution plumes. Because there is an identifiable need for a finer resolution aerosol product from MODIS, the MODIS aerosol team is introducing a 3 km product as part of their Collection 6 delivery. The 3 km product will be a Level 2 product, available in its own files, MOD04_3K for Terra and MYD04_3K for Aqua, and offer a subset of the original parameters over both land and ocean. The product is created using similar structure, inversion methods and Look Up Tables as the basic 10 km Dark Target products. The differences arise only in the manner pixels are selected and grouped for retrieval. Because the MODIS Dark Target aerosol algorithms were designed with climate applications in mind and on a 10 km scale, they were constructed in such a way to suppress noise in the retrieval. The danger of applying a similar inversion scheme on a finer scale is the possibility of introducing noise.

In this paper we introduce the MODIS Dark Target 3 km product by reviewing the algorithm producing the 10 km product and detailing the changes that allow for retrieval at 3 km. Then we demonstrate the new product in side-by-side comparisons between

the 3 km and 10 km retrievals of the same scenes. Finally, we produce a limited validation of the new product based on collocations with ground-based sunphotometry on a global basis, but for only 6 months of Aqua data. A companion paper in this same special issue describes the application of the new product with greater detail across an urban/suburban landscape (Munchak et al., 2012).

2 MODIS aerosol retrieval at 10 km and 3 km resolution

The MODIS Dark Target aerosol algorithms are well-documented in the literature (Kaufman et al., 1997; Tanré et al., 1997; Remer et al., 2005, 2012; Levy et al., 2007a, b, 2012). Here we provide a short review in order to highlight the differences between the 10 km and 3 km algorithms.

The MODIS Dark Target aerosol algorithms are two separate algorithms, one applied over ocean and one over land. They operate on five-minute segments of MODIS along-orbit data, known as "granules". Over ocean, the inputs consist of the MODIS-measured geolocated radiances normalized to reflectance units in 7 wavelengths (0.55, 0.66, 0.86, 1.24, 1.38, 1.63 and 2.13 μm), total column ozone concentrations from the NOAA Office of Satellite Product Operations, total column precipitable water vapor from the National Center for Environmental Prediction (NCEP) reanalysis, the MODIS cloud mask (MOD/MYD35) and in Collection 6 the surface wind speed from NCEP. The over land algorithm uses the 0.47, 0.66, 0.86, 1.24, 1.38, 2.13 μm channels, the ozone concentrations, and the total column precipitable water vapor. The 1.38 μm channel is available at 1 km resolution and is used to mask clouds, not retrieve aerosol. The 0.66 and 0.86 μm channels are available at 0.25 km resolution, and the other channels are available at 0.5 km resolution. Over land the 0.66 and 0.86 channels are used at their native resolution to identify inland and ephemeral water sources, then these bands are averaged to 0.5 km to create collocated spectral data at 0.5 km resolution, over both land and ocean. Normally, one granule is composed of 2708 × 4060 pixels at this resolution.

2.1 The MODIS 10 km Dark Target aerosol retrieval

Before the MODIS pixels are organized into retrieval boxes gaseous correction is applied and individual pixels are marked for either the ocean retrieval or the land retrieval. Then, for the 10 km (nominal at nadir) retrieval, we organize the entire MODIS granule into groups of 20×20 pixels, which we refer to as "retrieval boxes". The left side of Fig. 1 illustrates a 10 km retrieval box outlined in magenta.

After organization, the first step is to select the pixels within the retrieval box to be used in the retrieval. The algorithm avoids clouds, ocean sediments, glint, snow, ice, inland water and bright surfaces. Clouds are identified by means of spatial variability, ratio and threshold tests with additional assistance from specific tests from the MOD/MYD35 product (Martins et al., 2002; Gao et al., 2003; Frey et al., 2008; Remer et al., 2012). Sediments are identified in the ocean using spectral tests (Li et al., 2003) and sun glint is eliminated through the use of a 40° glint mask. Snow and ice are identified using spectral tests (Li, R-R. et al., 2005). Subpixel inland water is identified using the 0.66 and 0.86 µm channels and bright surfaces (> 0.25) at 2.13 µm are avoided altogether. After all unsuitable pixels are identified and deselected, the remaining pixels are sorted from lowest to highest reflectance at 0.86 µm over ocean and at 0.66 µm over land. The darkest and brightest 25 % of remaining pixels in the retrieval box are arbitrarily deselected over ocean, and the darkest 20 % and brightest 50 % of the remaining pixels are deselected over land. This means that in a 20×20 box, there are at most, 200 pixels over ocean or 120 pixels over land. In a 10 km retrieval box with 400 pixels even if many pixels are avoided for one or more of the above reasons or arbitrarily deselected at the dark or bright end of the distribution, there may still exist sufficient uncontaminated pixels to represent aerosol conditions in that box (Remer et al., 2012, this issue). The ocean algorithm requires 10 out of the 400 pixels at the 0.86 µm channel and at least 30 pixels total distributed across channels 0.55, 0.66, 1.24, 1.63 and 2.13 µm to represent aerosol conditions and to produce a high quality retrieval in that box. The

land algorithm requires 51 pixels in the 0.66 µm channel, for a high quality retrieval, but only 12 pixels for a degraded quality retrieval.

After the selection procedure if there are sufficient pixels remaining, the mean spectral reflectance is calculated from the remaining pixels. From the 400 pixels in the retrieval box, there emerges a single set of spectral reflectance representing the cloud-free conditions in the box. The spectral reflectances are matched in a Look Up Table with pre-calculated values. Over ocean the entries in the Look Up Table are calculated assuming a rough ocean surface, and in Collection 6 there are separate Look Up Tables for different surface wind speeds as determined from the NCEP wind data (Kleidman et al., 2012; Levy et al., 2012). Over land, the surface reflectance is constrained by spectral functions relating the visible to 2.13 µm (Levy et al., 2007a).

2.2 The 3 km retrieval

The only differences between the 3 km algorithm and the 10 km algorithm are the way the pixels are organized and the number of pixels required to proceed with a retrieval after all masking and deselection are accomplished. Figure 2 presents a flow chart showing the separate paths for the 10 km and 3 km retrievals. The black boxes running along the center of chart identify processes that are identical in both retrievals. The inputs are identical, as are the masking procedures. The exact same 0.5 km pixels identified as cloud, sediment etc. in the 10 km algorithm are identified as cloud, sediment etc. in the 3 km algorithm. The difference is in how the two algorithms make use of these 0.5 km designations. Once the 3 km algorithm has identified the pixels suitable for retrieval and decided that a sufficient number of these pixels remain, the spectral reflectances are averaged and the inversion continues exactly the same as in the 10 km algorithm. The same assumptions are used, the same Look Up Tables, the same numerical inversion and the same criteria to determine a good fit.

In the 3 km retrieval the 0.5 km pixels are arranged in retrieval boxes of 6 × 6 arrays of 36 pixels, illustrated by the schematic in the right hand side of Fig. 1. Note that in the 3 km retrieval box, the exact same pixels identified as cloudy in the 10 km retrieval

MODIS 3 km aerosol product: algorithm and global perspective

L. A. Remer et al.

Title Page

Abstract | Introduction

Conclusions | References

Tables | Figures

|◄ | ►|

◄ | ►

Back | Close

Full Screen / Esc

Printer-friendly Version

Interactive Discussion

box (denoted by the white rectangles) are identified as cloudy in the 3 km box. This is because both algorithms apply identical criteria to masking undesirable pixels. The 3 km retrieval attempts to apply similar deselection of pixels at the darkest and brightest ends of the distribution: 25 % and 25 % over ocean, and 20 % and 50 % over land. Once these darkest and brightest pixels are discarded, the algorithm averages the remaining pixels to represent conditions in the 3 km retrieval box. The algorithm requires a minimum of 5 pixels at 0.86 µm over ocean with at least 12 pixels distributed over the other five channels and 5 pixels are required over land in order to continue and make a retrieval. This is actually a more stringent requirement for ocean (14 % of 36), than what is required by the 10 km retrieval (2.5 %) for the best quality retrieval. The requirement over land is about the same in the 3 km retrieval as it is in the 10 km retrieval (14 % and 13 %, respectively).

Tables 1 through 3 list the parameters available in the MOD04_3K and MYD04_3K files. Not all of the diagnostics available at 10 km are included at 3 km, but most of the parameters are there. The data set includes an integer Quality Flag (Land_Ocean_Quality_Flag) that designates each 3 km retrieval as "3", "2", "1" or "0". The same recommendations apply to the 3 km product as to the original product. Ocean retrievals are valid for all nonzero Quality Flags while land retrieval products are only recommended for Quality Flags = "3". The 3 km product also includes more detailed diagnostics about the retrieval embedded in the Quality_Assurance_Ocean and Quality_Assurance_Land parameters. Note, that the criteria to fill these quality diagnostics differ slightly from the criteria used to fill the same-named parameters at 10 km. Detailed information on the quality diagnostics will be available in the Collection 6 Algorithm Theoretical Basis Document available at http://modis-atmos.gsfc.nasa.gov/reference_atbd.html.

The 3 km product is designed to provide insight into the aerosol situation on a focused local basis and will not be aggregated to the Level 3 global 1-degree grid. All Level 3 MODIS aerosol products will be derived from the 10 km product.

The 3 km retrieval should closely mirror the results of the 10 km retrieval because the majority of the two algorithms are identical, but it should be able to resolve gradients across the 10 km retrieval box that would otherwise be missed. There is a possibility that the new algorithm will introduce additional noise, especially over land where pixels representing inhomogeneous surfaces would have been eliminated in the deselection process of the larger box, but are now included in the retrieval. However, this tendency towards noise may be mitigated by the slightly more stringent requirements in deselection and the minimum number of pixels needed to represent the box. The advantageous mitigation features will be more apparent over ocean than over land. Overall, the two algorithms provide different sampling of the aerosols over the globe and because of this alone, are not expected to provide the same global statistics.

3 Examples of results from 3 km algorithm

The 3 km algorithm was applied to six months of MODIS data from Aqua-MODIS: January and July 2003, 2008 and 2010. This is a special database of MODIS data used to test new MODIS algorithms before implementation into operational production. The input radiances and MOD/MYD35 cloud mask are not final versions that appear or will appear in a publicly available data Collection, but the inputs are traceable within the MODIS processing environment. In Figs. 3–6, we show examples from Day 183, 15 July 2008 and from Day 12, 12 January 2010 that illustrate the new 3 km product and how it differs from the 10 km product applied to exactly the same input data.

Figure 3 compares the 10 km and 3 km ocean retrievals at over the Mediterranean Sea off the coast of Tunisia and Libya during a moderate dust event. The two resolution products produce almost the exact same aerosol field with the same gradient and same magnitude aerosol optical depth. This is because the two algorithms are essentially the same. The only difference is that the finer resolution product is able to make retrievals closer to the small islands in the image. We find that this is typical of the

3 km product. It offers over-ocean retrievals closer to land, nearer to islands and within narrow waterways and estuaries.

Figures 4 illustrate the apparent advantage of the 3 km product to resolve smoke plumes from fires. The fire is a large wild fire burning in Canada. The 10 km product does not capture the long narrow smoke plume leading towards the northwest, but the 3 km product does. One of the major advantages of the 3 km product is its ability to better resolve smoke plumes than the 10 km product. Even so, because the cloud identification algorithm in the 3 km product is the same as in the 10 km product, based primarily on spatial variability, the 3 km product still improperly confuses the thickest parts of the smoke plume with a cloud and mistakenly refuses to retrieve there.

Figure 5 demonstrates the potential for different sampling by the two products. The situation is a highly polluted episode over much of southeastern China. Here the 3 km algorithm makes retrievals over a broad area, while the 10 km algorithm finds few opportunities to retrieve. The few places of overlap result in similar values of aerosol optical depth. The only AERONET station in the image is at Hong_Kong_PolyU (22°18′, 114°11′), which reports a collocated AOD interpolated to 0.55 µm at MODIS overpass time of 0.38. The 10 km algorithm does not produce a retrieval at this station, but the 3 km algorithm does, producing an AOD of 0.45, a reasonable match. The collocation procedure and quantification of expected uncertainties are described in Sect. 5 below.

Figure 6 shows a potential concern of switching indiscriminately to the 3 km product. In this retrieval over the highly urbanized surface of Los Angeles and environs, the surface is incompatible with the current version of the Dark Target retrieval. The seasoned pixel selection process of the 10 km algorithm is able to recognize this incompatibility and chooses not to retrieve over Los Angeles. However, the 3 km product does retrieve, and the result is a scattering of retrieved AOD > 0.8 over the region. Although there is no ground truth to determine whether these points are accurate high AOD situations or noisy artifacts of the retrieval, it is highly likely that they are artifacts that the 3 km retrieval fails to avoid. Although the results of the 3 km product mirror the 10 km retrievals, we do find an increase of noisy artifacts in the finer resolution product. Unfortunately

this occurs most frequently over urban surfaces, a type of location of most interest to the air quality community.

4 Global mean aerosol statistics of the 3 km product

The global mean aerosol optical depth calculated from the 10 km and 3 km algorithms are different because the two algorithms sample differently. In general the global statistics of the 3 km product tracks the day-to-day variation of the 10 km product. Figure 7 shows the day-to-day global mean AOD differences between the two products over ocean and land for the three months of January merged into one continuous time series for plotting purposes and the three July months merged into another. A positive difference indicates that the 3 km AOD is higher than the 10 km AOD. The differences in global monthly mean AOD between the two resolution data sets is −0.004 in January and nearly 0.000 in July over ocean and 0.003 in January and 0.010 in July over land. The largest day to day differences between the products is seen over land in January, where daily differences can be either positive or negative. Because of snow cover over the northern land masses in January there are relatively fewer retrievals contributing to the global mean AOD, causing relatively larger day-to-day fluctuations over land in this month as compared with July. The large daily difference in the products in January over land, corresponding to Day 12 on 2010 on the graph (12 January 2010) does not correspond to an unusual spike in global land AOD, just to a large difference between the two products. On this day the differences are concentrated in a handful of granules, of which the most dramatic is the 05:35 UTC granule shown in Fig. 5. Likewise other spikes on the difference plots are not associated with unusual global mean AOD.

Figure 8 shows the scatter plots of the 3 km daily global mean over land and ocean plotted against the same using the 10 km product. Januarys and Julys are denoted by different symbols. The correlation between the two resolutions over land in July is very high ($R = 0.997$) with a regression equation slope approaching 1 and offset of only 0.015. There is greater deviation between the two resolutions in global mean statistics

on a day-by-day basis over land in January and over ocean in both months, but the correlation remains high ($R > 0.95$). January land is noisiest with the lowest correlation, most likely due to the snow cover and senescent vegetation of the northern temperate latitudes that severely reduces the number of retrievals on any day. As we see in Fig. 5, the two resolution algorithms are affected differently by these less than optimal surface conditions resulting in significantly different samples from which to construct the global mean. The result is the lower correlation of Fig. 8. Over ocean in January, the 3 km product tends to produce lower global mean AOD than the 10 km product. In July the tendency for lower global mean AOD is seen in the lower AOD range, but there is a strong positive slope in the regression equation so that when 10 km AOD is greater than 0.12, the 3 km product actually tends towards higher AOD. As of now we do not have an explanation for these tendencies in the global mean AOD statistics over ocean.

Figure 9 shows the histograms calculated from the six months of data described in Sect. 3, with all Januarys combined and all Julys combined, land and ocean separately. These histograms are constructed from individual retrieval boxes accumulated for the entire three-month periods with no spatial or diurnal averaging. The histograms are plotted with relative frequency rather than total number of retrievals in each bin because the 3 km product at finer spatial resolution produces approximately 11 times and 7 times the number of retrievals produced by the 10 km product, over land and ocean, respectively. Here we see over land with the 3 km product a decrease in the proportion of negative and very low AOD retrievals and an increase in retrievals in the 0.05–0.15 range in January and in the 0.15–0.35 range in July. This shift is more apparent in Fig. 10. The overall increase in global mean AOD over land with the 3 km product noted in Figs. 7 and 8 appears to be due to shifting to moderate AOD from very low AOD and not from introducing spikes at very high AOD. In contrast, over ocean the histograms show an increase in very low AOD (0–0.05) at the expense of slightly higher AOD (0.05–0.15 or 0.20). Figure 10 clarifies the differences between the 3 km and 10 km histograms.

Overall the 3 km product tracks the 10 km product on a day-to-day basis, although the product over land tends to be higher than the 10 km product, and over the ocean lower. There is seasonal variation to these tendencies.

5 Global validation

The six months of test data described above (January and July 2003, 2008 and 2010) were collocated with Level 2.0 AERONET observations to test the accuracy of the retrievals. For the 10 km retrievals we use the Petrenko et al. (2012) protocol for collocations, which differs slightly from the one introduced in Ichoku et al. (2002). Here, a collocation is the spatio-temporal average of all AERONET AOD measurements within ±30 min of MODIS overpass and the spatial average of all MODIS retrievals within a 25 km radius around the AERONET station. At nadir, the 25 km radius can encompass roughly 25 MODIS retrieval boxes, each at 10 km. However, MODIS pixel resolution increases with scan angle, as does the size of the retrieval boxes. At swath edges, the aerosol product box can be approximately 40 km instead of 10 km. The collocation protocol still calls for a 25 km radius, which now encompasses only parts of 4 boxes. To be included in the analysis, a 10 km collocation must include two AERONET observations within the hour and at least 20 % of the potential MODIS retrievals. This would be at least 5 out of 25 possible retrievals at nadir, but only 1 out of a possible 5 retrieval boxes towards the scan edge. For the 3 km retrievals we apply a 7.5 km radius around the AERONET stations, which encompasses 25 MODIS 3-km retrieval boxes at nadir. Again, for 3 km retrievals, we require at least 2 AERONET observations and 20 % of possible MODIS retrievals for the collocation to be included in the analysis. Note that the collocations are filtered using MODIS Quality Assurance (QA) flags. Only those MODIS retrievals with QA = 3 over land and QA > 0 over ocean within the 25 km or 7.5 km radius are included in the statistics of the collocation and the requirement is for at least 20 % of MODIS retrievals with acceptable QA for the collocation to be included in the analysis. The only wavelength examined is at 550 nm. This requires the

AERONET values to be interpolated to this wavelength in order to match MODIS. A quadratic fit in log-log space is used to make the interpolation (Eck et al., 1999).

Figure 11 shows the binned scatter plots from six months of collocations for land. There are 3298 collocations at 10 km and 3283 at 3 km. The data were sorted according to AERONET AOD and bins designated for every 50 collocations. The mean and standard deviation of both the AERONET and MODIS AODs were calculated. The mean values for each bin are plotted and the error bars indicate ±1 standard deviation. The red line represents the linear regression calculated for the full data set of over 3000 collocations and not the 66 bins plotted in the figure. The dashed lines indicate the "expected error" (Levy et al., 2010). For land the expected error is

$$\Delta AOD = \pm 0.05 \pm 0.15\, AOD$$

Table 4 provides the mean AOD of each data set, the correlation coefficient, the regression statistics and the number of MODIS retrievals that fall within expected error, fall above the expected error bound (the upper dashed line) and fall below the expected error bound (the lower dashed line in Fig. 11).

Figure 12 shows similar binned scatter plots for the ocean retrieval. There are fewer ocean collocations, 1100 at 10 km and 697 at 3 km. Because AERONET stations are generally on land, the 10 km retrieval with its longer radius will intercept more ocean retrievals than the 3 km retrieval with only a 7.5 km radius. The expected error for ocean is

$$\Delta AOD = \pm 0.03 \pm 0.05\, AOD.$$

These figures show that the 10 km product of this six-month database is meeting its expectations with most retrievals falling within expected error (71 % over land and 69 % over ocean). Correlations are high (0.87 over land and 0.93 over ocean) and most retrievals and the linear regression fall close to the 1:1 line. The land retrieval does show a positive bias of ∼ 0.015 and the ocean ∼ 0.005, but these are well-within expected uncertainties.

82

The 3 km product is also highly correlated to AERONET observations and most of the 3 km retrievals fall within the expected error bounds. However, the 3 km product matches AERONET less well than does the 10 km MODIS product. The most obvious degradation of accuracy between the 3 km and 10 km products is over land where the

5 finer resolution product has more than doubled its positive bias. This can be seen in Fig. 11 where the red cluster of points and regression line are now above the green 1:1 line. The ocean retrieval has also significantly increased its positive bias against AERONET at finer resolution. In addition to the increased bias the 3 km product introduces additional noise at low AOD. This can be seen in Fig. 12, where bin standard

10 deviations have increased, especially in the two lowest bins.

The positive bias in the MODIS-AERONET collocations is best seen in Fig. 13, where the difference in each bin has been plotted against AERONET AOD, separately for each product resolution, land and ocean. The x-axis in the figure has been truncated at AERONET AOD = 0.6 to emphasize the lower AOD range. Over ocean, the lowest

15 bins show a large relative increase in AOD bias, but for most of the AOD range the 3 km and 10 km biases against AERONET are approximately the same. Over land, the positive bias in the 3 km AOD exceeds 0.05 from AERONET AOD = 0.15 to 0.50.

Because AERONET stations used in the ocean validation collocations are limited to coastal and island stations they do not provide adequate sampling over the open

20 ocean where most of the ocean retrievals take place. The Maritime Aerosol Network is a relatively new network under the AERONET umbrella that offers quality-assured AOD measurements from ships of opportunity over the open ocean (Smirnov et al., 2009). We identified collocations between the MAN AOD and the Aqua-MODIS 10 km and 3 km retrievals during the six months of this test data set, January and July, 2003, 2008

25 and 2010. A collocation was defined using the same spatial averaging and minimum number of MODIS retrieval criteria as with a MODIS-AERONET collocation. The MAN measurements temporally average a series of measurements together to form one measurement. All "series" measurements within a half hour of the MODIS overpass are temporally averaged. Due to the limited amount of MAN data, there was no minimum

Title Page

Abstract | Introduction

Conclusions | References

Tables | Figures

|◀ | ▶|

◀ | ▶

Back | Close

Full Screen / Esc

Printer-friendly Version

Interactive Discussion

number of MAN "series" measurements required to create a collocation. Only ocean retrievals with a QA $\geq$ 1 are included in the collocation. Because of the requirement that there be at least 20 % of available retrievals within a 7.5 km radius for the 3 km product and a 25 km radius for the 10 km product, the two sets of collocations do not necessarily

5 contain the same points. In our sets of MAN-MODIS collocations both the 3 km and 10 km retrievals contain 37 points, of which 27 are the same and 10 are unique for each resolution. The AERONET collocation exercise also results in differently sampled data sets, but the results of this different sampling is much more apparent in the MAN process because of the small statistical sampling size.

10 The results of the MODIS-MAN collocations are shown in Fig. 14. Most MAN collocations occurred in very clean environments with the exception of 3 points (only 2 at 10 km) that occurred in the tropical Atlantic in the dust belt and a moderate value near AOD $\sim$ 0.2 from the Hudson Bay that appears to be wildfire smoke. The highest AOD collocation in the 3 km data base (9 July 2008 from the dust belt of the Atlantic Ocean

15 with MODIS AOD = 0.67) does not appear in the 10 km data base. Most of the MODIS 3 km points agree with the MAN observations to within expectations. The exceptions include that one high dust point and a group of collocations at low AOD that are all traced to a specific cruise within sight of the Antarctic coast in January 2008. The regression and correlation statistics are given in Fig. 14 and in Table 4 but because of the outlying

20 dust point in the 3 km set, these statistics are not robust descriptions of the bulk of the observations. For example while the mean AODs of the MAN and MODIS populations are 0.077 and 0.101, respectively, the medians are 0.051 and 0.059, respectively. The 37 points are inadequate to fully represent the relationship between MODIS 3 km retrievals over the wide variety of conditions experienced over the world's oceans. They

25 are shown here to supplement the other inadequate data set of the AERONET coastal and island sites. Together the available ocean validation does suggest, without firm proof, that the ocean 3 km retrieval will achieve similar levels of uncertainty as the well-studied ocean 10 km product.

6 Discussion and conclusions

The MODIS Dark Target aerosol algorithm relies on a data selection process that identifies a relatively few ideal pixels to use in the retrieval of aerosol optical depth and other aerosol characteristics. By choosing only a few pixels to represent aerosol over a moderate resolution retrieval box, noise is reduced and situations difficult to retrieve are avoided. Inherent in this selection procedure is an assumption that aerosol properties do not vary across the retrieval box, so that the aerosol conditions across the box can be represented by just a small fraction of pixels. Except for specific situations near sources: smoke plumes from fires, dust plumes from playas, etc., aerosol homogeneity over mesoscale lengths of 40–400 km has been considered to be a robust assumption (Anderson et al., 2003). The 10 km (nadir) to 40 km (swath edge) retrieval is a reasonable algorithm construct, given this understanding of aerosol homogeneity. However, as our opportunities to observe aerosols increase and our understanding grows, we know now that aerosol may vary frequently over much smaller spatial scales (Shinozuka and Redemann, 2011; Munchak et al., 2012 this issue). Not only will the 10 km retrieval box lose the details of local variability, the assumption on which it is based may be in error.

Because there is need for finer resolution aerosol products to resolve individual plumes and fine gradients, the MODIS Science Team is introducing a 3 km product in their Collection 6 delivery. This product will be available at the granule level, in separate files labeled as MOD04_3K and MYD04_3K, for Terra and Aqua, respectively. The new product differs from the original 10 km product only in the manner in which reflectance pixels are ingested, organized and selected by the aerosol algorithm. All cloud, surface, sediment, snow and ice masking remain identical to the original algorithm, and Look Up Tables and inversion methods have not changed. The only difference is in how the algorithm arbitrarily discards additional *good* pixels to obtain the *best* pixels for retrieval. In the 3 km algorithm, pixels will be used for retrieval that would have been arbitrarily discarded by the 10 km algorithm.

Title Page

Abstract | Introduction

Conclusions | References

Tables | Figures

|◄ | ►|

◄ | ►

Back | Close

Full Screen / Esc

Printer-friendly Version

Interactive Discussion

The 3 km product exhibits expected characteristics. It resolves aerosol plumes and details of fine-scale gradients that the 10 km product misses. In some situations it provides retrievals over entire regions that the 10 km barely samples. The 3 km product also allows the ocean retrieval to retrieve closer to islands and in narrow bays. On the other hand, in situations known to be difficult for the Dark Target retrieval, such as over bright surfaces and especially over urban surfaces, the 3 km retrieval introduces sporadic unrealistic high values of AOD that are avoided more successfully by the 10 km retrieval. We can label these artifacts as "noise", but it is not random noise because the tendency over land is to over estimate AOD in these artifacts.

Over land, globally, the 3 km product appears to be 0.01 to 0.02 higher than the 10 km product. There are strong differences between January and July, indicative of a seasonal shift, but with only 6 months of data over 3 yr to analyze, the seasonal pattern cannot be resolved. The fact that over land AOD is higher in the 3 km product than in the 10 km product could be due to the fact that the finer resolution product retrieves in strong aerosol plumes, missed by the coarser resolution product. This would suggest that the 3 km global mean AOD is a truer representation of the global mean. On the other hand, the 3 km product introduces a high-biased noise over bright and/or urban surfaces, and so, the global mean from the 10 km product would remain the truer representation. Collocations with AERONET observations suggest the latter. The 3 km AOD over land compares less well with AERONET than does the 10 km AOD, decreasing correlation, increasing high bias and shifting retrievals from within expectations of uncertainty to exceeding those expectations. We conclude that the 3 km AOD over land is less accurate and less robust than the 10 km AOD. Estimated uncertainty of the 3 km land product, based on 6 months of collocations with AERONET, suggest that 67 % of retrievals should fall within

$$\Delta AOD\_3\,km = \pm0.05 \pm 0.25\,AOD$$

with the understanding that most retrievals will fall within the positive end of this error bounding, leaving a positive bias.

Over ocean, globally, the 3 km algorithm picks up proportionally a greater number of very low AOD cases than the 10 km algorithm. Again, just from comparing the two MODIS resolution products we cannot tell whether this low bias is a better representation of global AOD or not. Unfortunately, the comparison with AERONET cannot either.

AERONET stations used for the over ocean validation are isolated to a limited number of island and coastal locations. The very low AOD situations tend to occur over open ocean. The AERONET analysis suggests that the 3 km algorithm introduces positive bias, not negative. This is because the 3 km product retrieves closer to shore, where the AERONET station is located. In these locations, likelihood of sediment contamination is high, aerosol is continental in nature and we expect that the result of the AERONET validation over ocean is not applicable to the global oceanic AOD retrieval. We cannot even conclude about the relative accuracy of the two products in the coastal zone, because the validation procedure enables the 10 km product to encompass retrievals much further from shore than the 3 km product. However, in the coastal zone, within 7.5 km of shore, we conclude that 69 % of 3 km retrievals should fall within

$$\Delta AOD\_3\,km = \pm 0.03 \pm 0.05\,AOD$$

with caution expressed for the lowest AOD situations, which appear to be randomly noisier than the expressed uncertainty bound.

The data from the MAN cruises were also inadequate to state firm conclusions about the 3 km ocean retrieval because only 37 collocations were identified in the analysis data set, and several of those points were highly localized to specific locations such as Hudson Bay and near the Antarctic coast. However, even in this limited data set, 68 % of the 3 km retrievals were contained within the error bounds stated above for the ocean retrieval.

All analysis presented in this paper represent Aqua-MODIS from a limited 6 month analysis data set. Terra-MODIS data from the same 6 months were also examined subsequently, and no results from the Terra analysis contradict the conclusions presented here.

We have made no attempt in this analysis to address cloud effects on the 3 km retrieval. Some of the high bias seen in the over land product could be due to additional cloud contamination and cloud effects in the product instead of artifacts introduced by bright surfaces. However, the fact that the ocean 3 km product does not also contain this high bias prompts us towards considering surface effects and not clouds, but without further analysis we cannot make firm conclusions. Definitely future work will need to address cloud 3-D effects (Wen et al., 2007; Marshak et al., 2008), the so-called twilight zone or continuum (Koren et al., 2007; Charlson et al., 2007) and other cloud issues on the finer resolution aerosol product.

Overall the 3 km product mimics the 10 km product, globally, and on a granule-by-granule basis. Because the new product is essentially the same as the traditional Dark Target product, it is well-understood and the limited analysis presented above is sufficient to recommend its use by the community with the following caveats:

– Global studies should continue to make use of the more robust and well-studied 10 km product. The 3 km product's use should be restricted to obvious situations that require finer resolution.

– Only the AOD at 550 nm was examined in this study. Differences in the spectral AOD and size parameter retrievals over ocean in the two resolution products are possible.

– Aerosol-cloud studies with the 3 km product should proceed cautiously. At this time, we do not know specifically how the 3 km product is affected in the proximity of clouds.

– While the air quality community will be eager to apply the 3 km product across an urban landscape, this must proceed cautiously because of known artifacts in the product over urban surfaces. See Fig. 6 and Munchak et al. (2012 this issue).

The power of the new product is on the local scale, not the global one, as was studied here. Future work that applies the MODIS 3 km aerosol product to local aerosol

situations in case studies and evaluates the results will be necessary to continue the work started here (i.e. Munchak et al., 2012). We expect the new 3 km product to provide important information complementary to existing satellite-derived products and become an important tool for the aerosol community.

References

Al-Saadi, J., Szykman, J., Pierce, R. B., Kittaka, C., Neil, D., Chu, D. A., Remer, L., Gumley, L., Prins, E., Weinstock, L., MacDonald, C., Wayland, R., Dimmick, F., and Fishman, J.: Improving national air quality forecasts with satellite aerosol observations, Bull. Am. Meteorol. Soc., 86, 1249–1264, doi:10.1175/BAMS-86-9-1249, 2005.

Anderson, T. L., Charlson, R. J., Winker, D. M., Ogren, J. A., and Holmen, K.: Mesoscale variations of tropospheric aerosols, J. Atmos. Sci., 60, 119–136, doi:10.1175/1520-0469(2003)060<0119:MVOTA>2.0.CO;2, 2003.

Castanho, A. D. D., Martins, J. V., and Artaxo, P.: MODIS aerosol optical depth Retrievals with high spatial resolution over an urban area using the critical reflectance, J. Geophys. Res.-Atmos., 113, D02201, doi:10.1029/2007JD008751, 2008.

Charlson, R. J., Ackerman, A. S., Bender, F. A.-M., Anderson, T. L., and Liu, Z.: On the climate forcing consequences of the albedo continuum between cloudy and clear air, Tellus B, 59, 715–727, doi:10.1111/j.1600-0889.2007.00297.x, 2007.

Christopher S. A., Zhang, J., Kaufman, Y. J., and Remer, L. A.: Satellite-based assessment of top of atmosphere anthropogenic aerosol radiative forcing over cloud-free oceans, Geophys. Res. Lett., 33, L15816, doi:10.1029/2005GL025535, 2006.

Chu, D. A., Kaufman, Y. J., Zibordi, G., Chern, J. D., Mao, J., Li, C., and Holben, B. N.: Global monitoring of air pollution over land from EOS- Terra MODIS, J. Geophys. Res., 108, 4661, doi:10.1029/2002JD003179, 2003.

Eck, T. F., Holben, B. N., Reid, J. S., Dubovik, O., Smirnov, A., O'Neill, N. T., Slutsker, I., and Kinne, S.: Wavelength dependence of the optical depth of biomass burning, urban and desert dust aerosols, J. Geophys. Res., 104, 31333–31350, 1999.

Engel-Cox, J. A., Holloman, C. H., Coutant, B. W., and Hoff, R. M: Qualitative and quantitative evaluation of MODIS satellite sensor data for regional and urban scale air quality, Atmos. Environ., 38, 2495–2509, doi:10.1016/j.atmosenv.2004.01.039, 2004.

Title Page

Abstract | Introduction

Conclusions | References

Tables | Figures

|◄ | ►|

◄ | ►

Back | Close

Full Screen / Esc

Printer-friendly Version

Interactive Discussion

Frey, R. A., Ackerman, S. A., Liu, Y., Strabala, K. I., Zhang, H., Key, J., and Wang, X.: Cloud Detection with MODIS, Part I: Recent Improvements in the MODIS Cloud Mask, JTECH.25, 1057–1072, 2008.

Gao, B.-C., Kaufman, Y. J., Tanre, D., and Li, R.-R.: Distinguishing tropospheric aerosol from thin cirrus clouds for improved aerosol retrievals using the ratio of 1.38 µm and 1.24 µm channels, Geophys Res. Lett., 29, 1890, doi:10.1029/2002GL015475, 1890.

Hsu, N. C., Tsay, S. C., King, M. D., and Herman, J. R.: Aerosol properties over bright-reflecting source regions, IEEE Trans. Geosci. Remote Sens., 42, 557–569, doi:10.1109/TGRS.2004.824067, 2004.

Ichoku, C., Chu, D. A., Mattoo, S., Kaufman, Y. J., Remer, L. A., Tanré, D., Slutsker, I., and Holben, B. N.: A spatio-temporal approach for global validation and analysis of MODIS aerosol products, Geophys. Res. Lett., 29, 1616, doi:10.1029/2001GL013206, 2002.

Kaufman, Y. J., Tanré, D., Remer, L. A., Vermote, E. F., Chu, A., and Holben, B. N.: Operational remote sensing of tropospheric aerosol over land from EOS moderate resolution imaging spectroradiometer, J. Geophys. Res., 102, 17051–17067, 1997.

Kaufman, Y. J., Tanre, D., and Boucher, O.: A satellite view of aerosols in the climate system, Nature, 419, 215–223, 2002.

Kaufman, Y. J., Boucher, O., Tanré, D., Chin, M., Remer, L. A., and Takemura, T.: Aerosol anthropogenic component estimated from satellite data, Geophys. Res. Lett., 32, L17804, doi:10/1029/2005, 2005a.

Kaufman, Y. J., Koren, I., Remer, L. A., Tanré, D., Ginoux, P., and Fan, S.: Dust transport and deposition observed from the Terra-MODIS spacecraft over the Atlantic Ocean, J. Geophys. Res., 110, D10S12, doi:10.1029/2003JD004436, 2005b.

Kaufman, Y. J., Koren, I., Remer, L. A., Rosenfeld, D., and Rudich, Y.: The Effect of Smoke, Dust and Pollution Aerosol on Shallow Cloud Development Over the Atlantic Ocean, Proc. Natl. Acad. Sci., 102, 11207–11212, 2005c.

Kinne, S., Schulz, M., Textor, C., Guibert, S., Balkanski, Y., Bauer, S. E., Berntsen, T., Berglen, T. F., Boucher, O., Chin, M., Collins, W., Dentener, F., Diehl, T., Easter, R., Feichter, J., Fillmore, D., Ghan, S., Ginoux, P., Gong, S., Grini, A., Hendricks, J., Herzog, M., Horowitz, L., Isaksen, I., Iversen, T., Kirkevåg, A., Kloster, S., Koch, D., Kristjansson, J. E., Krol, M., Lauer, A., Lamarque, J. F., Lesins, G., Liu, X., Lohmann, U., Montanaro, V., Myhre, G., Penner, J., Pitari, G., Reddy, S., Seland, O., Stier, P., Takemura, T., and Tie, X.: An AeroCom initial

AMTD

6, 69–112, 2013

MODIS 3 km aerosol product: algorithm and global perspective

L. A. Remer et al.

Title Page	
Abstract	Introduction
Conclusions	References
Tables	Figures

◄◄	►►
◄	►
Back	Close

Full Screen / Esc

Printer-friendly Version

Interactive Discussion

assessment – optical properties in aerosol component modules of global models, Atmos. Chem. Phys., 6, 1815–1834, doi:10.5194/acp-6-1815-2006, 2006.

Kleidman, R. G., Smirnov, A., Levy, R. C., Mattoo, S., and Tanré, D.: Evaluation and wind speed dependence of MODIS aerosol retrievals over open ocean, IEEE Trans. Geosci. Remote Sens., 50, 429–435, doi:10.1109/TGRS.2011.2162073, 2012.

Koren, I. and Wang, C.: Cloud-rain interactions: as complex as it gets, Environ. Res. Lett., 3, 045018, doi:10.1088/1748-9326/3/4/045018, 2008.

Koren, I., Kaufman, Y. J., Rosenfeld, D., Remer, L. A., and Rudich, Y.: Aerosol invigoration and restructuring of Atlantic convective clouds, Geophys. Res. Lett., 32, 014005, doi:10.1029/2005GL023187, 2005.

Koren, I., Remer, L. A., Kaufman, Y. J., Rudich, Y., and Martins, J. V.: On the twilight zone between clouds and aerosols, Geophys. Res. Lett., 34, L08805, doi:10.1029/2007GL029253, 2007.

Levy, R. C, Remer, L. A., Mattoo, S., Vermote, E. F., and Kaufman, Y. J.: A second-generation algorithm for retrieving aerosol properties over land from MODIS spectral reflectance, J. Geophys. Res., 112, D13211, doi:10.1029/2006JD007811, 2007a.

Levy, R. C., Remer, L. A., and Dubovik, O.: Global aerosol optical properties and application to Moderate Resolution Imaging Spectroradiometer aerosol retrieval over land, J. Geophys. Res., 112, D13210, doi:10.1029/2006JD007815, 2007b.

Levy, R. C., Remer, L. A., Kleidman, R. G., Mattoo, S., Ichoku, C., Kahn, R., and Eck, T. F.: Global evaluation of the Collection 5 MODIS dark-target aerosol products over land, Atmos. Chem. Phys., 10, 10399–10420, doi:10.5194/acp-10-10399-2010, 2010.

Levy, R. C., Mattoo, S., Munchak, L. A., Remer, L. A., Sayer, A., and Hsu, N. C.: The Collection 6 MODIS aerosol products over land and ocean, Atmos. Meas. Tech., in press, 2012.

Li, C. C., Lau, A. K. H., Mao, J. T., and Chu, D.A.: Retrieval, validation, and application of the 1-km aerosol optical depth from MODIS measurements over Hong Kong. IEEE Trans. Geosci. Remote Sens., 43, 2650–2658, doi:10.1109/TGRS.2005.856627, 2005.

Li, R.-R., Kaufman, Y. J., Gao, B.-C., and Davis, C. O.: Remote sensing of suspended sediments and shallow coastal waters, IEEE Trans. Geosci. Remote Sens., 41, 559–566, 2003.

Li, R.-R., Remer, L., Kaufman, Y. J., Mattoo, S., Gao, B.-C., and Vermote. E.: Snow and Ice Mask for the MODIS Aerosol Products, IEEE Trans. Geosci. Remote Sens. Lett., 3, 306–310, 2005.

Title Page

Abstract | Introduction

Conclusions | References

Tables | Figures

|◄ | ►|

◄ | ►

Back | Close

Full Screen / Esc

Printer-friendly Version

Interactive Discussion

Loeb, N. G. and Schuster, G. L.: An observational study of the relationship between cloud, aerosol and meteorology in broken low-level cloud conditions, J. Geophys. Res., 113, D14214, doi:10.1029/2007JD009763, 2008.

Lyapustin, A., Wang, Y., Laszlo, I., Kahn, R., Korkin, S., Remer, L., Levy, R., and Reid, J.: Multi-angle implementation of atmospheric correction (MAIAC): Part 2. Aerosol algorithm, J. Geophys. Res.-Atmos., 116, D03211, doi:10.1029/2010JD014986, 2011.

Marshak, A., Wen, G., Coakley Jr., J. A., Remer, L. A., Loeb, N. G., and Cahalan, R. F.: A simple model for the cloud adjacency effect and the apparent bluing of aerosols near clouds, J. Geophys. Res., 113, D14S17, doi:10.1029/2007JD009196, 2008.

Martins, J. V., Tanré, D., Remer, L. A., Kaufman, Y. J., Mattoo, S., and Levy, R.: MODIS Cloud Screening for Remote Sensing of Aerosol over Oceans using Spatial Variability, Geophys. Res. Lett., 29, 1619, doi:10.1029/2001GL013205, 2002.

Munchak, L. A., Levy, R. C., Mattoo, S., Remer, L. A., Holben, B. N., Schafer, J. S., Hostetler, C. A., and Ferrare, R. A.: MODIS 3 km aerosol product: Applications over land in an urban/suburban region, Atmos. Meas. Tech., in preparation, 2012.

Petrenko, M., Ichoku, C., and Leptoukh, G.: Multi-sensor Aerosol Products Sampling System (MAPSS), Atmos. Meas. Tech., 5, 913–926, doi:10.5194/amt-5-913-2012, 2012.

Redemann, J., Zhang, Q., Livingston, J., Russell, P., Shinozuka, Y., Clarke, A., Johnson, R., and Levy, R.: Testing aerosol properties in MODIS Collection 4 and 5 using airborne sunphotometer observations in INTEX-B/MILAGRO, Atmos. Chem. Phys., 9, 8159–8172, doi:10.5194/acp-9-8159-2009, 2009.

Remer, L. A., Kaufman, Y. J., Tanré, D., Mattoo, S., Chu, D. A., Martins, J. V., Li, R. R., Ichoku, C., Levy, R. C., Kleidman, R. G., Eck, T. F., Vermote, E., and Holben, B. N.: The MODIS aerosol algorithm, products and validation, J. Atmos. Sci., 62, 947–973, 2005.

Remer L., Tanré, D., and Kaufman, Y. J.: Algorithm for Remote Sensing of Tropospheric Aerosols from MODIS: Collection 5, Algorithm Theoretical Basis Document, available at: http://modis.gsfc.nasa.gov/data/atbd/atbd_mod02.pdf (last access: 19 December 2012), 2006.

Remer, L. A., Mattoo, S., Levy, R. C., Heidinger, A., Pierce, R. B., and Chin, M.: Retrieving aerosol in a cloudy environment: aerosol product availability as a function of spatial resolution, Atmos. Meas. Tech., 5, 1823–1840, doi:10.5194/amt-5-1823-2012, 2012.

Russell, P. B., Livingston, J. M., Redemann, J., Schmid, B., Ramirez, S. A., Ellers, J., Kahn, R., Chu, D. A., Remer, L., Quinn, P. K., Rood, M. J., and Wang, W.: Multi-grid-cell validation of

Title Page

Abstract | Introduction

Conclusions | References

Tables | Figures

|◀ | ▶|

◀ | ▶

Back | Close

Full Screen / Esc

Printer-friendly Version

Interactive Discussion

satellite aerosol property retrievals in INTEX/ITCT/ICARTT 2004, J. Geophys. Res.-Atmos., 112, D12S09, doi:10.1029/2006JD007606, 2007.

Shinozuka, Y. and Redemann, J.: Horizontal variability of aerosol optical depth observed during the ARCTAS airborne experiment, Atmos. Chem. Phys., 11, 8489–8495, doi:10.5194/acp-11-8489-2011, 2011.

Smirnov, A., Holben, B. N., Slutsker, I., Giles, D. M., McClain, C. R., Eck, T. F., Sakerin, S. M., Macke, A., Croot, P., Zibordi, G., Quinn, P. K., Sciare, J., Kinne, S., Harvey, M., Smyth, T. J., Piketh, S., Zielinski, T., Proshutinsky, A., Goes, J. I., Nelson, N. B., Larouche, P., Radionov, V. F., Goloub, P., Krishna Moorthy, K., Matarrese, R., Robertson, E. J., and Jourdin, F.: Maritime Aerosol Network as a component of Aerosol Robotic Network, J. Geophys. Res., 114, D06204, doi:10.1029/2008JD011257, 2009.

Stier, P., Feichter, J., Kinne, S., Kloster, S., Vignati, E., Wilson, J., Ganzeveld, L., Tegen, I., Werner, M., Balkanski, Y., Schulz, M., Boucher, O., Minikin, A., and Petzold, A.: The aerosol-climate model ECHAM5-HAM, Atmos. Chem. Phys., 5, 1125–1156, doi:10.5194/acp-5-1125-2005, 2005.

Tanré D., Kaufman, Y. J., Herman, M., and Mattoo, S.: Remote sensing of aerosol properties over oceans using the MODIS/EOS spectral radiances, J. Geophys. Res., 102, 16971–16988, 1997.

van Donkelaar, A., Martin, R. V., and Park, R. J.: Estimating ground-level PM(2.5) using aerosol optical depth determined from satellite remote sensing, J. Geophys. Res.-Atmos., 111, D21201, doi:10.1029/2005JD006996, 2006.

van Donkelaar, A., Martin, R. V., Brauer, M., Kahn, R., Levy, R., Verduzco, C., and Villeneuve, P. J.: Global Estimates of Ambient Fine Particulate Matter Concentrations from Satellite-Based Aerosol Optical Depth: Development and Application, Environ. Health Perspec., 118, 847–855, doi:10.1289/ehp.0901623, 2010.

Wang, J. and Christopher, S. A.: Intercomparison between satellite-derived aerosol optical thickness and PM2.5 mass: Implications for air quality studies, Geophys. Res. Lett., 30, 2095, doi:10.1029/2003GL018174, 2003.

Wen, G., Marshak, A., Cahalan, R. F., Remer, L. A., and Kleidman, R. G.: 3D aerosol-cloud radiative interaction observed in collocated MODIS and ASTER images of cumulus cloud fields, J. Geophys. Res, 112, D13204, doi:10.1029/2006JD008267, 2007.

Yu, H., Kaufman, Y. J., Chin, M., Feingold, G., Remer, L. A., Anderson, T. L., Balkanski, Y., Bellouin, N., Boucher, O., Christopher, S., DeCola, P., Kahn, R., Koch, D., Loeb, N., Reddy,

Title Page

Abstract | Introduction

Conclusions | References

Tables | Figures

|◄ | ►|

◄ | ►

Back | Close

Full Screen / Esc

Printer-friendly Version

Interactive Discussion

M. S., Schulz, M., Takemura, T., and Zhou, M.: A review of measurement-based assess-ments of the aerosol direct radiative effect and forcing, Atmos. Chem. Phys., 6, 613–666, doi:10.5194/acp-6-613-2006, 2006.

Yu, H. B., Remer, L. A., Chin, M., Bian, H. S., Kleidman, R. G., and Diehl, T.: A satellite-based assessment of transpacific transport of pollution aerosol, J. Geophys. Res.-Atmos., 113, D14S12, doi:10.1029/2007JD009349, 2008.

Yu, H., Remer, L. A., Chin, M., Bian, H., Tan, Q., Yuan, T., and Zhang, Y,: Aerosols from Overseas Rival Domestic Emissions over North America, Science, 337, 566–569, doi:10.1126/science.1217576, 2012.

Zhang, J.-L., Reid, J. S., Westphal, D., Baker, N., and Hyer, E.: A system for operational aerosol optical depth data assimilation over global oceans, J. Geophys. Res., 113, D10208, doi:10.1029/2007JD009065, 2008.

Title Page

Abstract | Introduction

Conclusions | References

Tables | Figures

|◄ | ►|

◄ | ►

Back | Close

Full Screen / Esc

Printer-friendly Version

Interactive Discussion

Table 1. Land and ocean parameters of the MOD/MYD04_3K file and the parameter's dimension.

Parameter	dimension
Longitude	(X,Y)
Latitude	(X,Y)
Scan_Start_Time	(X,Y)
Solar_Zenith	(X,Y)
Solar_Azimuth	(X,Y)
Sensor_Zenith	(X,Y)
Sensor_Azimuth	(X,Y)
Scattering_Angle	(X,Y)
Glint_Angle	(X,Y)
Land_Ocean_Quality_Flag	(X,Y)
Land_sea_Flag	(X,Y),
Optical_Depth_Land_And_Ocean	(X,Y)
Image_Optical_Depth_Land_And_Ocean	(X,Y)

(X,Y) refers to a 2-dimensional array along and across the swath.

Table 2. Ocean parameters of the MOD/MYD04_3K file and the parameter's dimension.

Parameter	dimension
Wind_speed_Ncep_Ocean	(X,Y)
Solution_Index_Ocean_Small	(X,Y)
Solution_Index_Ocean_Large	(X,Y)
Effective_Optical_Depth_Best_Ocean	(X,Y,7); 0.47, 0.55, 0.66, 0.86, 1.24, 1.63, 2.13 µm
Effective_Optical_Depth_Average_Ocean	(X,Y,7); 0.47, 0.55, 0.66, 0.86, 1.24, 1.63, 2.13 µm
Optical_Depth_Small_Best_Ocean	(X,Y,7); 0.47, 0.55, 0.66, 0.86, 1.24, 1.63, 2.13 µm
Optical_Depth_Small_Average_Ocean	(X,Y,7); 0.47, 0.55, 0.66, 0.86, 1.24, 1.63, 2.13 µm
Optical_Depth_Large_Best_Ocean	(X,Y,7); 0.47, 0.55, 0.66, 0.86, 1.24, 1.63, 2.13 µm
Optical_Depth_Large_Average_Ocean	(X,Y,7); 0.47, 0.55, 0.66, 0.86, 1.24, 1.63, 2.13 µm
Mass_Concentration_Ocean	(X,Y)
Aerosol_Cloud_Fraction_Ocean	(X,Y)
Effective_Radius_Ocean	(X,Y,2): best, average
PSML003	(X,Y,2): best, average
Asymmetry_Factor_Best_Ocean	(X,Y,7); 0.47, 0.55, 0.66, 0.86, 1.24, 1.63, 2.13 µm
Asymmetry_Factor_Average_Ocean	(X,Y,7); 0.47, 0.55, 0.66, 0.86, 1.24, 1.63, 2.13 µm
Backscattering_Ratio_Best_Ocean	(X,Y,7); 0.47, 0.55, 0.66, 0.86, 1.24, 1.63, 2.13 µm
Backscattering_Ratio_Average_Ocean	(X,Y,7); 0.47, 0.55, 0.66, 0.86, 1.24, 1.63, 2.13 µm
Angstrom_Exponent_1_Ocean (0.55/0.86 micron)	(X,Y,2): best, average
Angstrom_Exponent_2_Ocean (0.86/2.1 micron)	(X,Y,2): best, average
Least_Squares_Error_Ocean	(X,Y,2): best, average
Optical_Depth_Ratio_Small_Ocean_055micron	(X,Y,2): best, average
Optical_Depth_by_models	(X,Y,9): 9 models
Number_Pixels_Used_Ocean	(X,Y)
Mean_Reflectance_Ocean	(X,Y,7); 0.47, 0.55, 0.66, 0.86, 1.24, 1.63, 2.13 µm
STD_Reflectance_Ocean	(X,Y,7); 0.47, 0.55, 0.66, 0.86, 1.24, 1.63, 2.13 µm
Quality_Assurance_Ocean	(X,Y); Packed byte

X, Y refers to a 2-dimensional array along and across the swath. Some parameters have a third dimension. A dimension of "7" refers to the 7 retrieved ocean wavelengths, listed. A dimension of "2" refers to either the solution with minimum fitting error (best) or the average of all solutions with fitting error less than 3 % (average) (Remer et al., 2005). A dimension of "9" refers to the 9 models, 4 fine mode and 5 coarse mode, used in the retrieval (Remer et al., 2005).

Table 3. Land parameters of the MOD/MYD04_3K file and the parameter's dimension.

Parameter	dimension
Aerosol_Type_Land	(X,Y)
Fitting Error_Land	(X,Y)
Surface_Reflectance_Land	(X,Y,3); 0.47, 0.66, 2.13 μm
Corrected_Optical_Depth_Land	(X,Y,3*); 0.47, 0.55, 0.66 μm
Corrected_Optical_Depth_Landwav2p1	(X,Y)
Optical_Depth_Ratio_Small_Land	(X,Y)
Number_Pixels_Used_Land	(X,Y)
Mean_Reflectance_Land	(X,Y,7); 0.46, 0.55, 0.66, 0.86, 1.24, 1.63, 2.13 μm
STD_Reflectance_Land	(X,Y,7); 0.46, 0.55, 0.66, 0.86, 1.24, 1.63, 2.13 μm
Mass_Concentration_Land	(X,Y)
Aerosol_Cloud_Fraction_Land	(X,Y)
Quality_Assurance_Land	(X,Y)
Topographic_Altitude_Land	(X,Y)

X,Y refers to a 2-dimensional array along and across the swath.
Some parameters have a third dimension.
A dimension of "3" refers to the 3 wavelengths of input reflectances used in the retrieval, listed.
A dimension of "3*" refers to the 3 retrieved wavelengths over land, listed.
A dimension of "7" refers to the 7 solar wavelengths, listed.

Table 4. Parameters from MODIS-AERONET collocation validation: means of each data set, correlation coefficient, regression slope and offset, number of collocations, percent within expected error[*], percent above expected error[*] and percent below expected error[*], for 10 km abd 3 km products, separated into land and ocean retrievals. The last rows show MODIS-MAN collocations over ocean.

	AERONET or MAN Mean	MODIS Mean	R	Slope	offset	N	% EE	% above EE	% below EE
land 10 km	0.158	0.172	0.87	0.93	0.02	3298	71	18	11
land 3 km	0.153	0.200	0.84	1.04	0.04	3283	62	31	7
ocean 10 km	0.143	0.148	0.94	0.95	0.01	1100	69	20	11
ocean 3 km	0.139	0.156	0.90	0.96	0.02	697	69	24	7
Ocean 10 km MAN	0.072	0.094	0.93	1.04	0.02	37	65	35	0
	(median = 0.054)	(median = 0.064)							
Ocean 3 km MAN	0.077	0.101	0.94	1.21	0.01	37	68	30	2
	(median = 0.051)	(median = 0.059)							

[*] Expected error for land is $\pm 0.05 \pm 0.15$ AOD, and for ocean it is $\pm 0.03 \pm 0.05$ AOD.
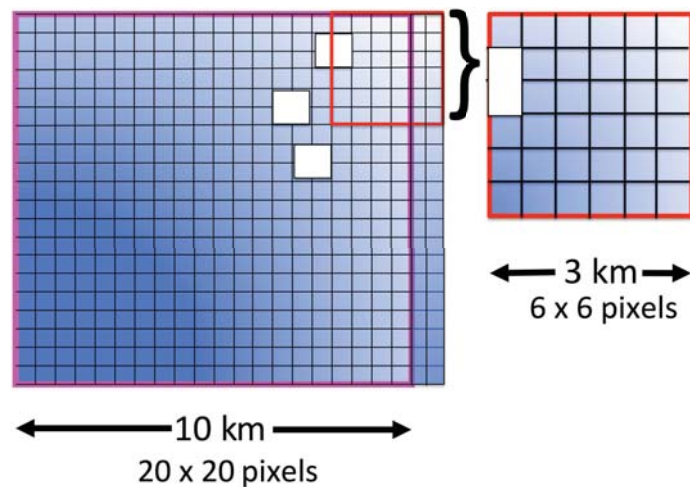
Fig. 1. Illustration of the organization of the MODIS pixels into retrieval boxes for (left) the 10 km product consisting of 20×20 0.5 km pixels within the magenta square and (right) the 3 km product consisting of 6×6 0.5 pixels within the red square. The small blue squares represent the 0.5 km pixels. The white rectangles represent pixels identified as cloudy. The 3 km retrieval box is independent of the 10 km box, and is not a subset. Here it is shown enlarged.
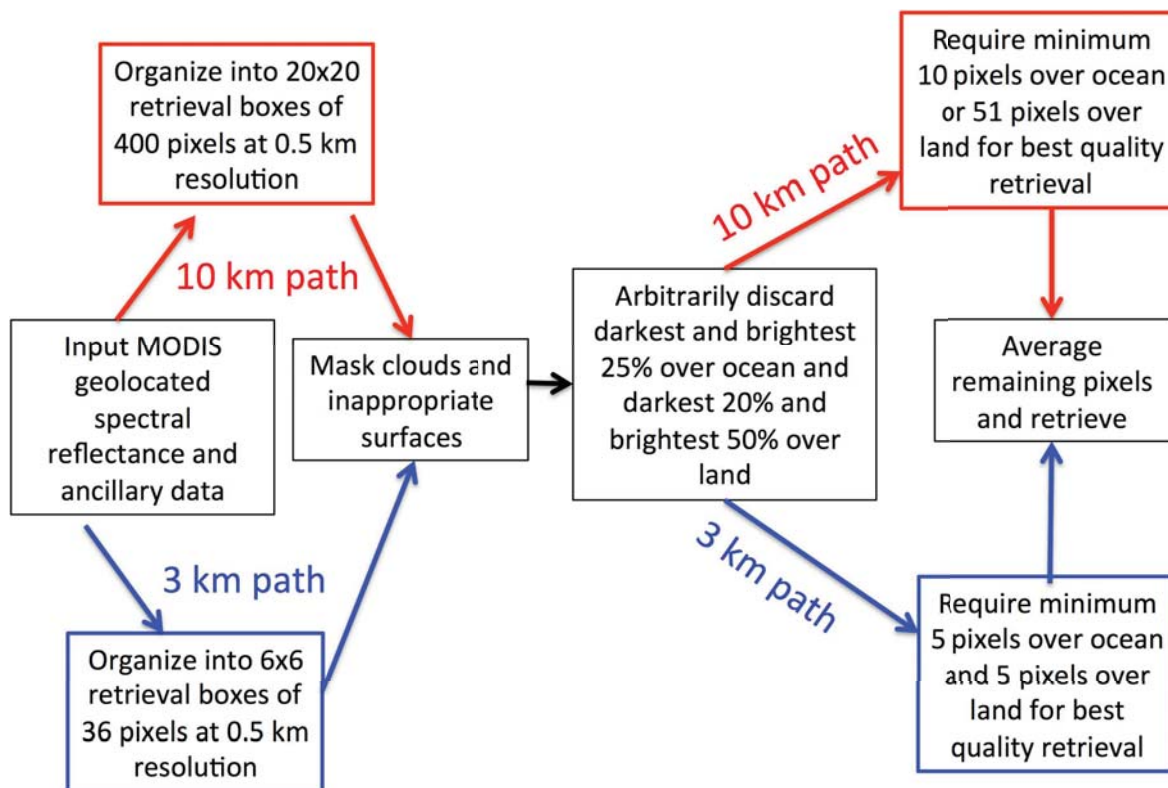
Fig. 2. Flowchart illustrating the different paths of the 10 km (red) and 3 km (blue) retrievals. The procedures appearing in the black outlined boxes are common to both algorithms.

Full Screen / Esc

Printer-friendly Version

Interactive Discussion

(a) 10 km, 13:00 UTC   **(b) 3 km, 13:00 UTC**

AOD at 550 nm

-0.05   0.05   0.15   0.25   0.35   0.45   0.55   0.65   0.75
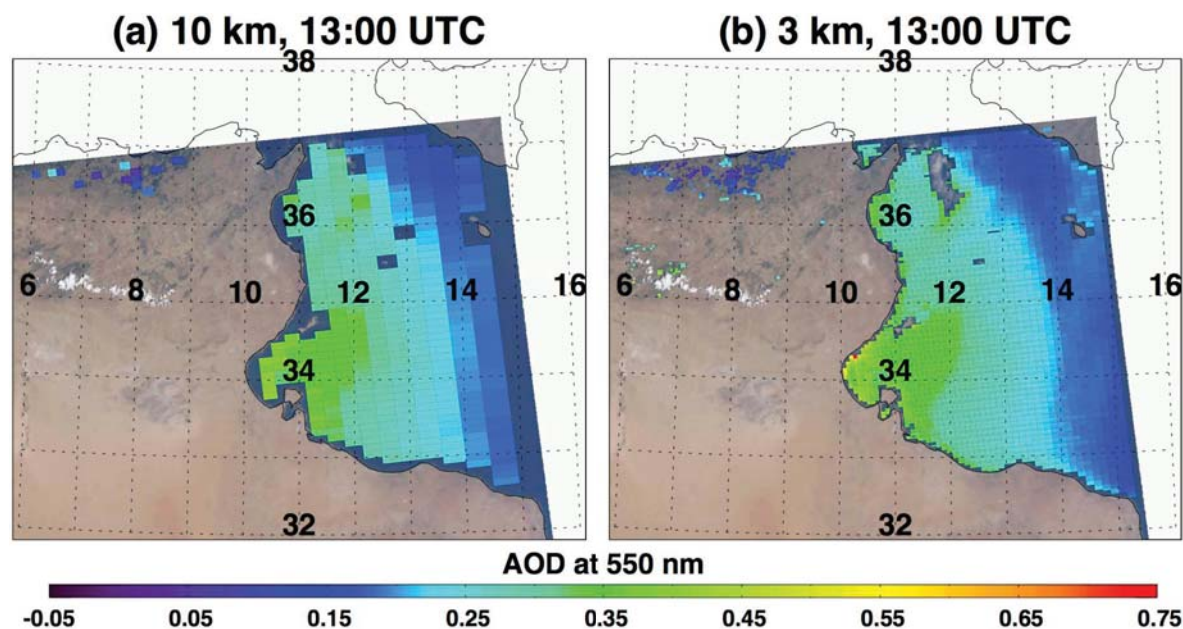
Fig. 3. Aerosol optical depth at 550 nm retrieved from the 15 July 2010 Aqua-MODIS radiances using the Collection 6 MODIS Dark Target aerosol algorithm. Left: the product at 10 km resolution. Right: the product at 3 km resolution. The situation is a moderate dust event over the Mediterranean Sea off the costs of Tunisia and Libya. The 3 km retrieval produces values closer to the coastline and to the islands.
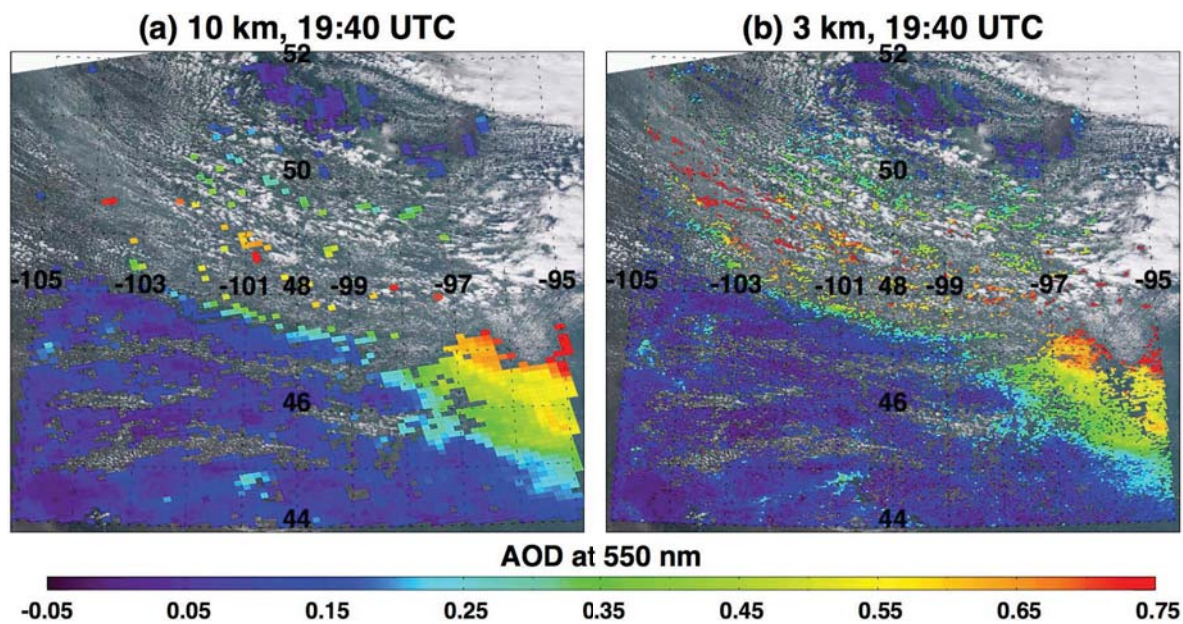
Fig. 4. Same as Fig. 3 but for a situation over Canada where the 3 km product better resolves the plume from active wildfires. Note the additional red pixels between the clouds in the upper left corner of the image for the 3 km panel.
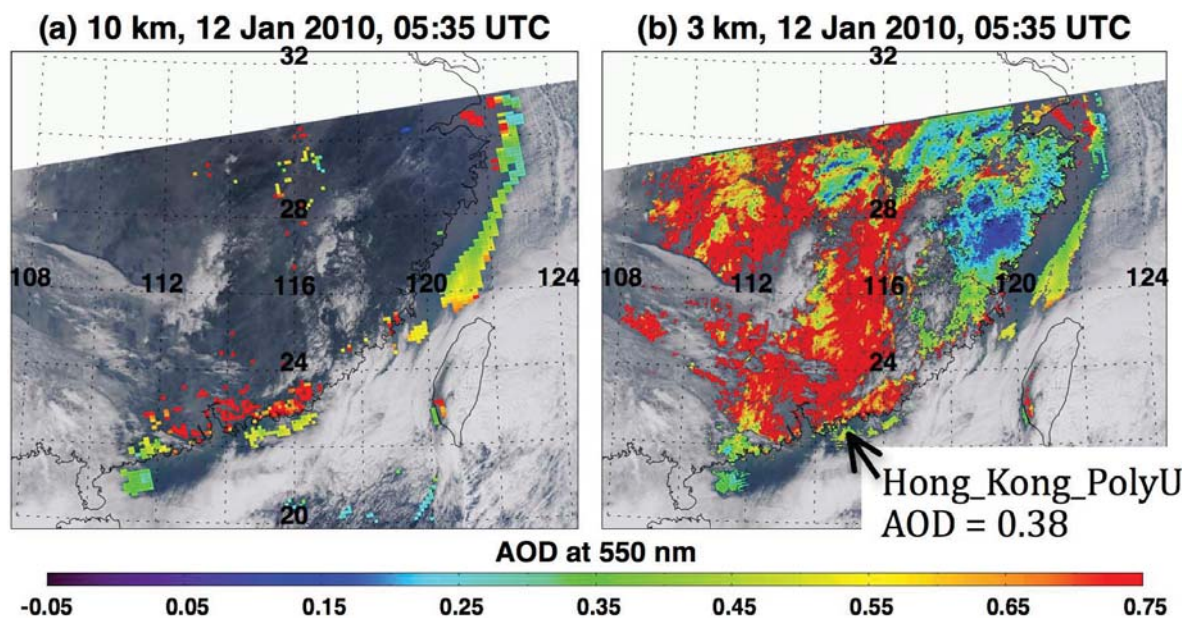
Fig. 5. Same as Fig. 3, but for 12 January 2010 during a pollution episode in China. Here the 3 km algorithm is able to make retrievals over a much broader region. The AOD interpolated to 0.55 μm from the only AERONET station in the image (Hong_Kong_PolyU) is 0.38. The 3 km retrieval there is 0.45, while there is no 10 km retrieval available at that spot during this overpass.

(a) 10 km, 21:15 UTC

(b) 3 km, 21:15 UTC

Urban artifacts

AOD at 550 nm

-0.05   0.05   0.15   0.25   0.35   0.45   0.55   0.65   0.75
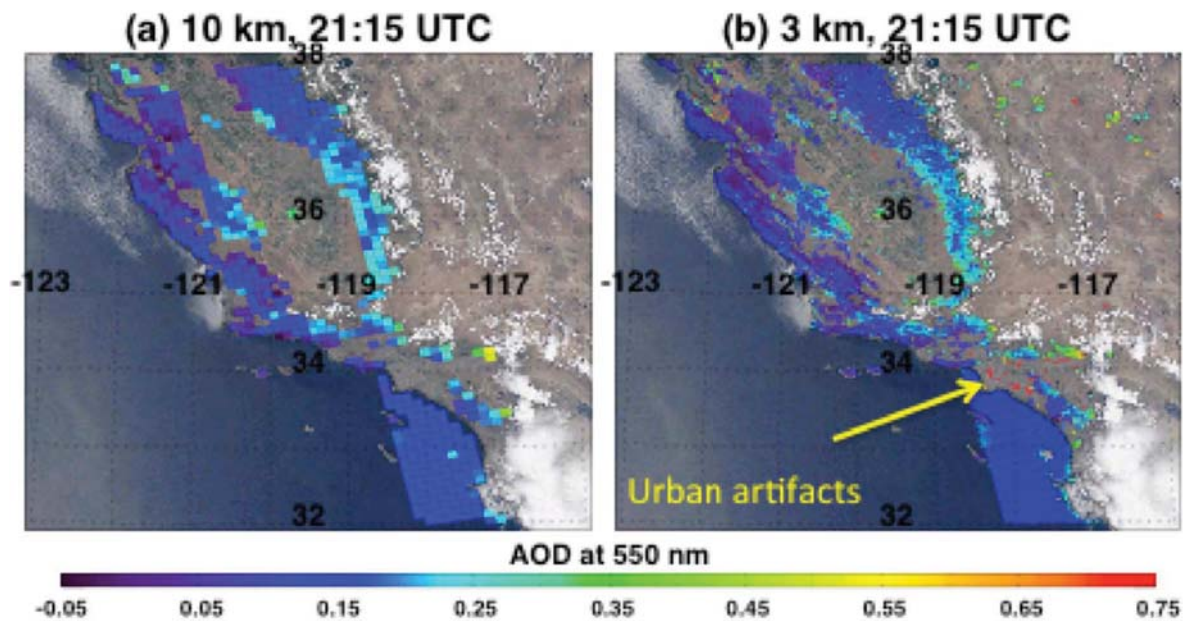
Fig. 6. Same as in Figure 3 but for a situation over California where the 3 km product introduces artificial noise over an urban area that the 10 km product avoids.
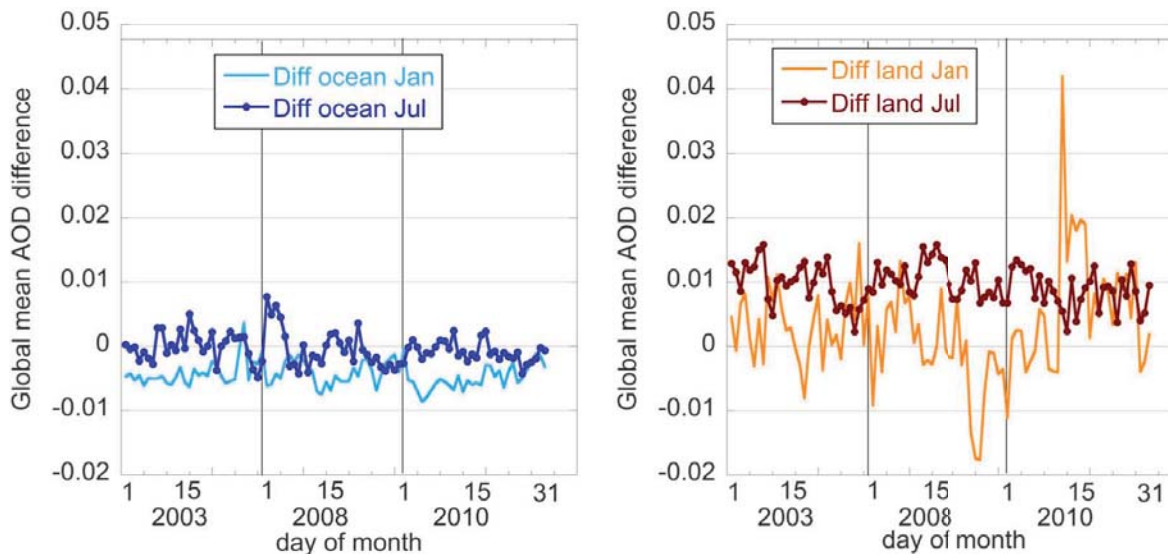
Fig. 7. Difference between 3 km daily global mean aerosol optical depth (AOD) at 550 nm and the same at 10 km for over ocean (left) and over land (right). Positive differences indicate that the 3 km AOD is higher than the 10 km AOD.
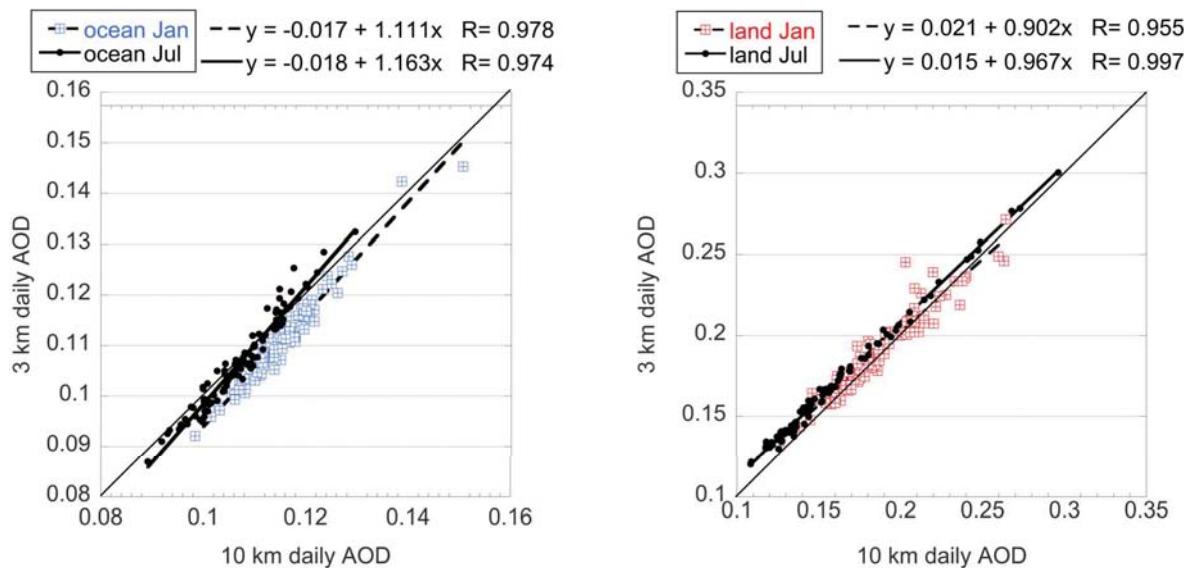
Fig. 8. Daily global mean aerosol optical depth (AOD) at 550 nm for the 93 days of the Januarys, and 93 days of the Julys 2003, 2008 and 2010 calculated from the 3 km product plotted against the same calculated using the 10 km product. The left plot is for ocean, and the right plot is for land.
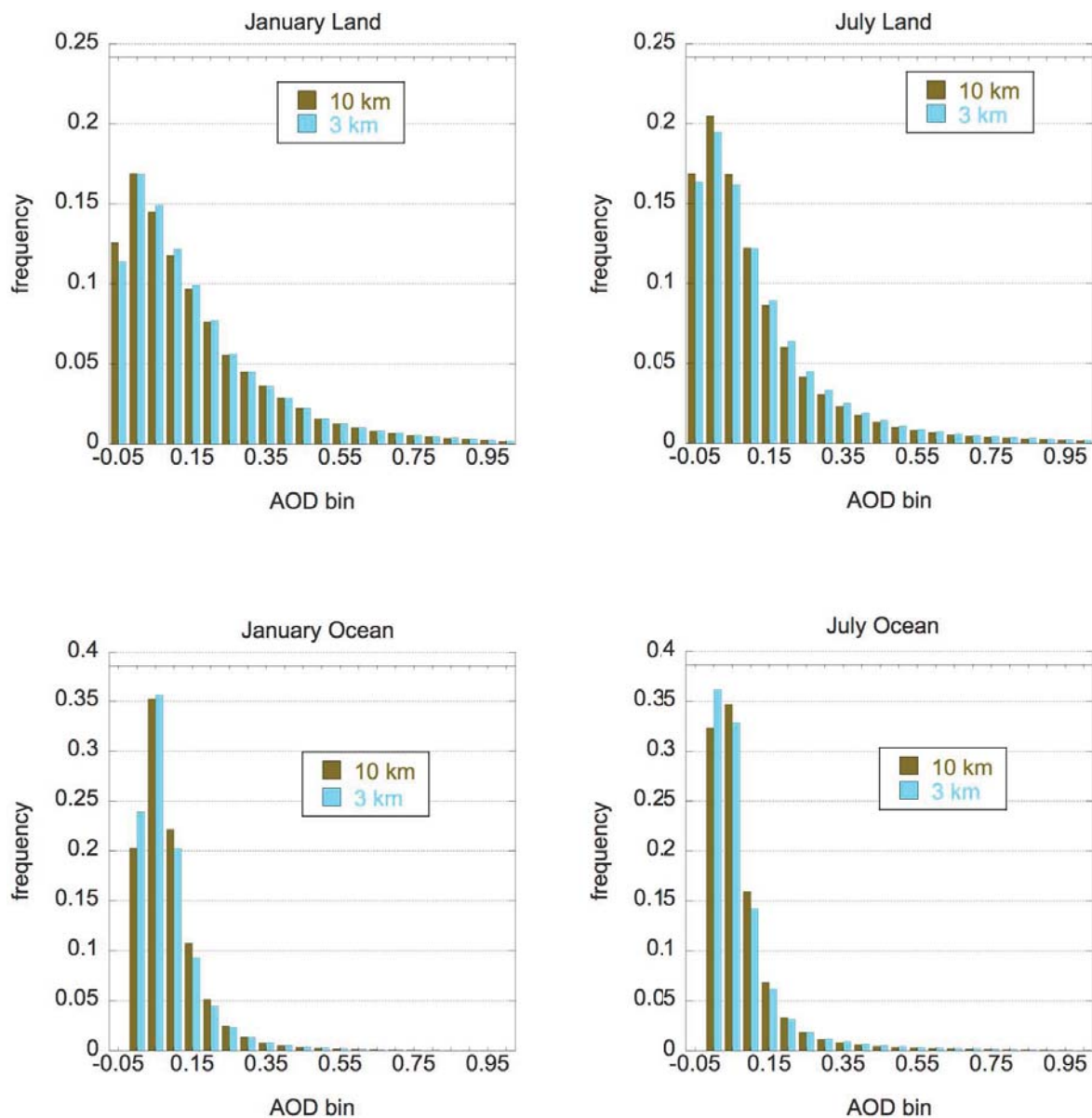
Fig. 9. Frequency histograms of 10 km and 3 km AOD retrievals, constructed from global retrievals from three Januarys (2003, 2008 and 2010) in the left column and from three Julys (same years) in the right column. Land in the top row and ocean in the bottom.
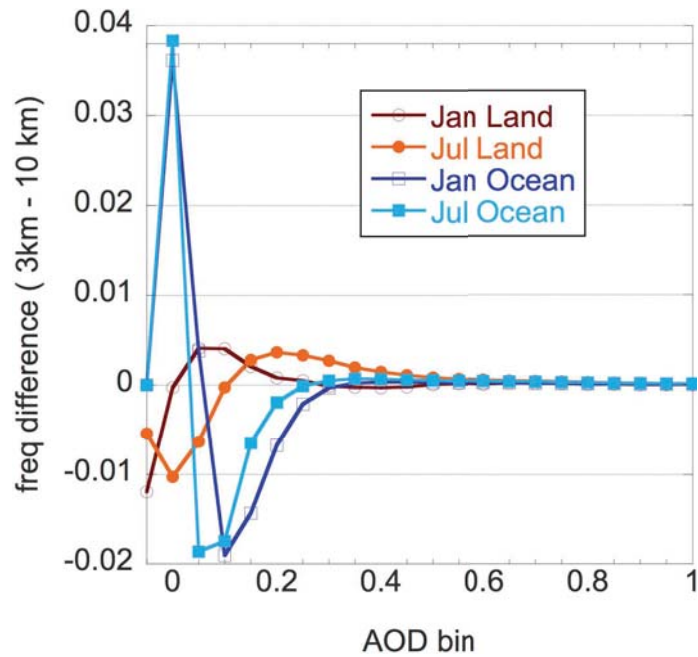
Fig. 10. Bin by bin differences between the frequency histograms of Fig. 9 (3 km–10 km).
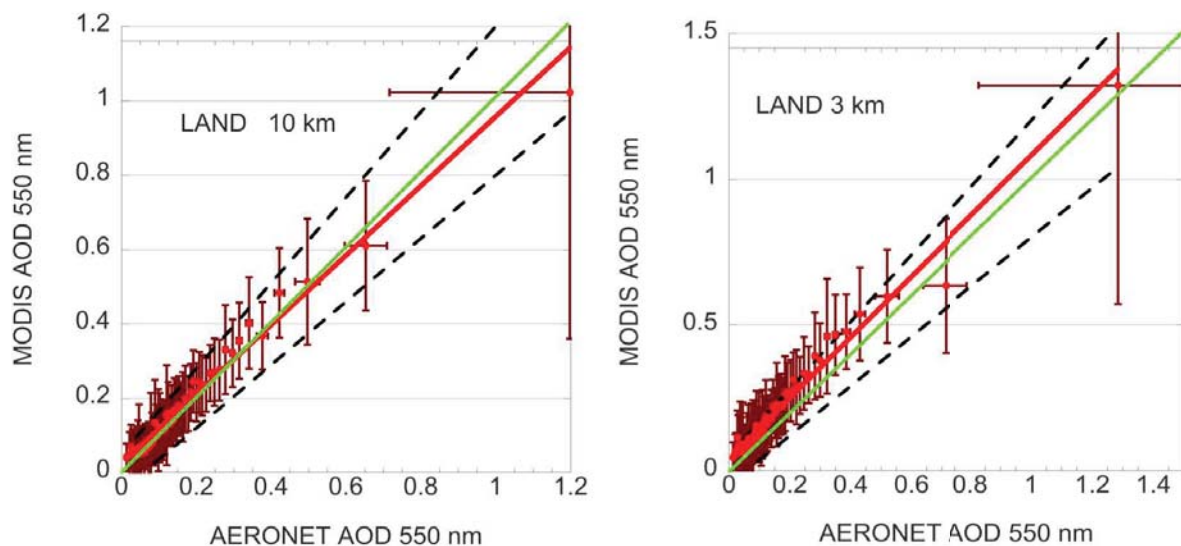
Fig. 11. Binned scatter plot of MODIS AOD at 550 nm retrieved from over land against AERONET observed AOD. MODIS 10 km product on the left and 3 km product on the right. Each bin represents 50 collocations. AERONET AOD has been interpolated to this wavelength to match MODIS. Error bars represent ±1 standard deviation in the bin. The green line is the 1:1 line. The red line is the linear regression through the full database of 3298 and 3283 collocations for 10 km and 3 km, respectively. The dashed lines represent expected error of the MODIS 10 km retrieval. Regression statistics are given in Table 4.
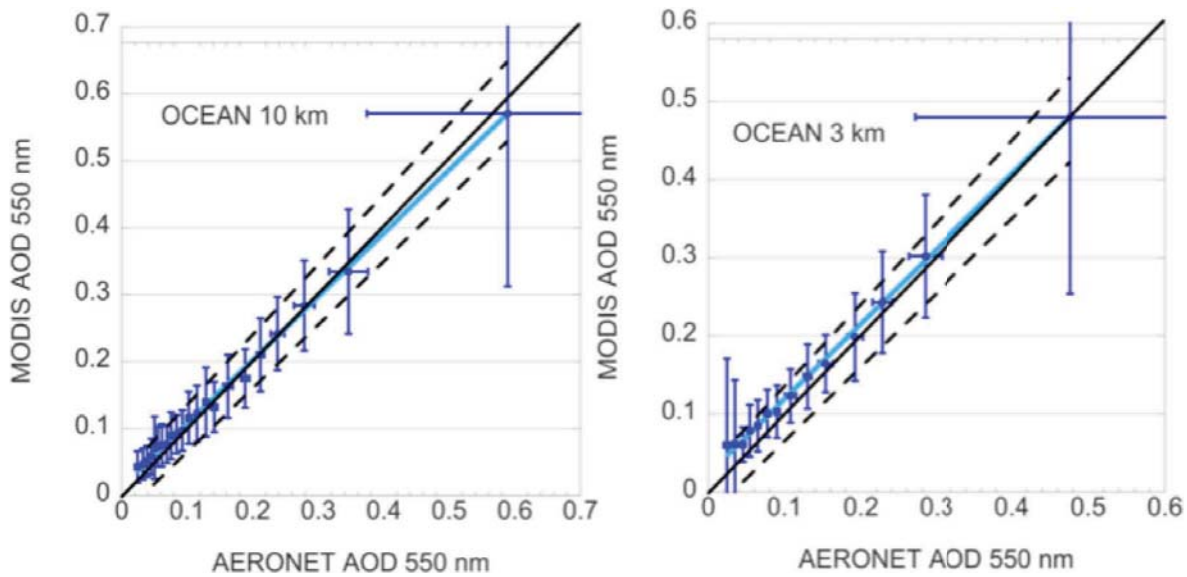
Fig. 12. Same as Fig. 11, but for over ocean retrieval. Here, the linear regression line is in light blue and the 1:1 line is in black.
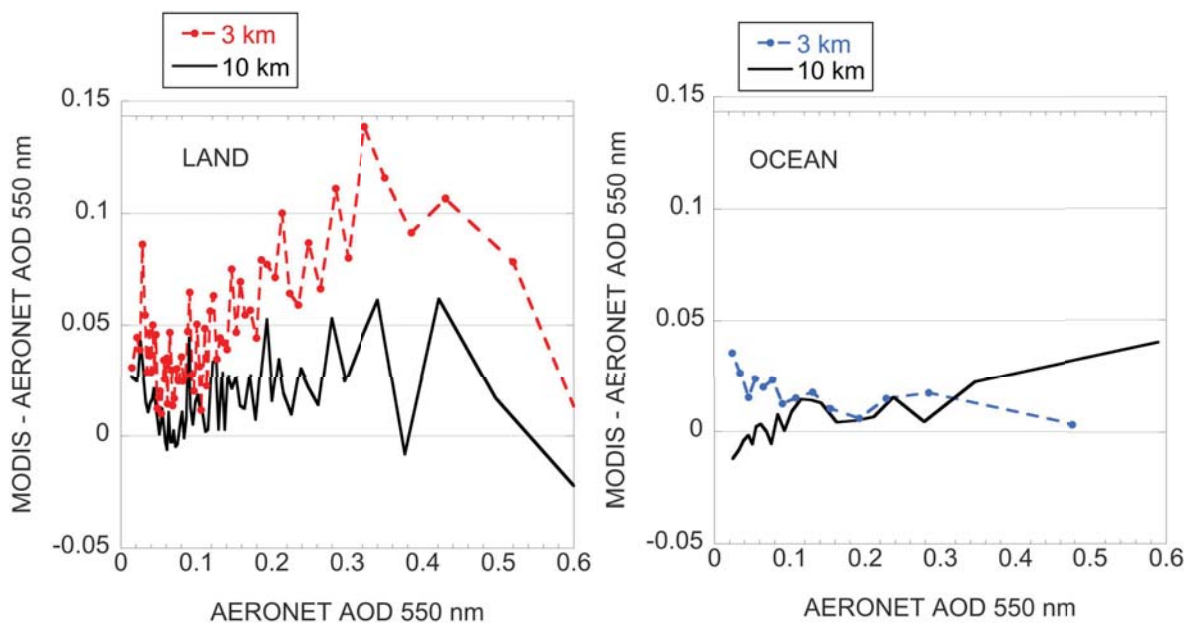
Fig. 13. Binned differences of MODIS – AERONET AOD 550 nm plotted as a function of AERONET AOD. Land is on the left and ocean on the right. 3 km products are denoted by dashed lines and 10 km products by solid lines. The x-axis has been truncated at AOD = 0.6 to emphasize the lower AOD bins.
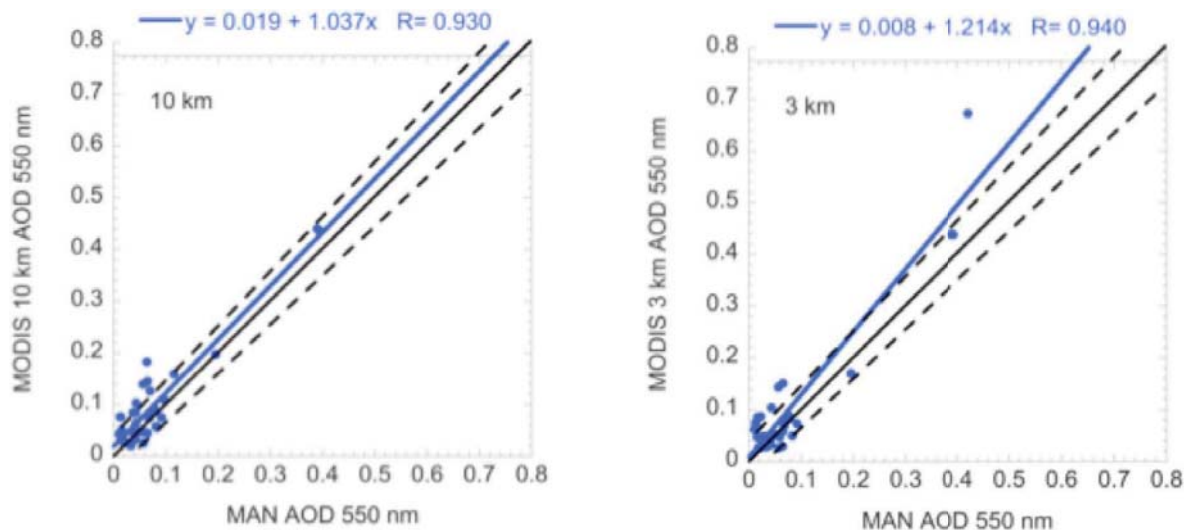
Fig. 14. Scatter plot of MODIS 10 km and 3 km retrievals of AOD at 550 nm plotted against collocated data from the Maritime Aerosol Network (MAN). 37 collocations were identified at each resolution in the 6 months undergoing analysis, although they are not necessarily the same 37 days in each plot.